A Modulation-Defined RF Micro-Acoustic Delay Line based on ScAlN MEMS Resonators for Self-Interference Cancellation

Giuseppe Michetti[#], Sasank Garikapati[$], Meruyert Assylbekova[#], Harish Krishnaswamy[$], Matteo Rinaldi[#]
[#]ECE, Northeastern University, USA
[$]EE, Columbia University, USA
michetti.g@northeastern.edu

***Abstract*— We present and demonstrate a time-modulated tunable bandwidth (BW) and group-delay (GD) filter, exploring a slow-modulation operating region of N-path filters to extend the BW of conventional passive micro-acoustic filters. An array of MEMS resonators is fabricated with custom in-house ScAlN process, and heterogeneously integrated on PCB with commercial RF switches to showcase ultra-low modulation frequency, 2 to 6 % of the filter center frequency, with wide maximum BW (11.6 % with a k_t^2 =2.5 % at 430 MHz), three-fold wider than passive topologies, enabling reconfiguration while requiring no tunable passive. We show that the proposed prototype is suitable as a Self-Interference Canceler (SIC) in full-duplex scenarios, where real-time GD tunability is required. When used as an SIC, 40 dB SI cancellation within 14 % BW is achieved. Thanks to the slow-modulation approach, a 17 dBm power handling is demonstrated, along with a low −28 dBc distortion.**

I. Introduction

Full-duplex wireless communication allows for a more efficient usage of the wireless spectrum. However, it requires cancellation of large amounts of self-interference (SI) signal leaking from the transmitter to receiver [1], [2]. Circuits known as SI cancellers are used to tap a portion of TX signal and inject it back into the receiver with appropriate phase and magnitude scaling to cancel the SI.

Achieving wideband SI cancellation requires emulating the frequency response of the highly dispersive SI channel for the entire bandwidth [3]. Thus, the canceller should also have a tunable and dispersive frequency response with sufficient group delay. Such a canceler can be implemented by having multiple delay taps with variable gain amplifiers (VGA) and phase shifters whose signals are combined to obtain a dispersive frequency response. The gains and phases of the VGAs and phase shifters can be tuned appropriately, realizing an FIR filter with a response matching that of the frequency response of the channel. Having large delays in the taps enables higher cancellations as they can capture the finer variations in the frequency response of the SI channel.

Conventional passive ladder delay-elements based on MEMS resonators[4], require frequency trimming between the series resonator and the shunt resonator resonance frequencies, typically in the few percent order, set by k_t^2, leaving little design room for BW enhancement, as k_t^2 is typically set by MEMS mode excitation.

In this work, we propose a time-variant modulation-defined filter (MDF), capable of synthesizing a wide-band response with tunable group delay (GD) and fractionally low modulation frequency (f_m),thanks to the strategic use of custom designed RF MEMS resonators, relaxing constraints on k_t^2 requirements for wide-band operation. As $f_m \ll f_{res}$, the circuit operation completely differs from N-path circuits [5], [6], rather operating in a delay element region of operation for sequentially switched circuits.

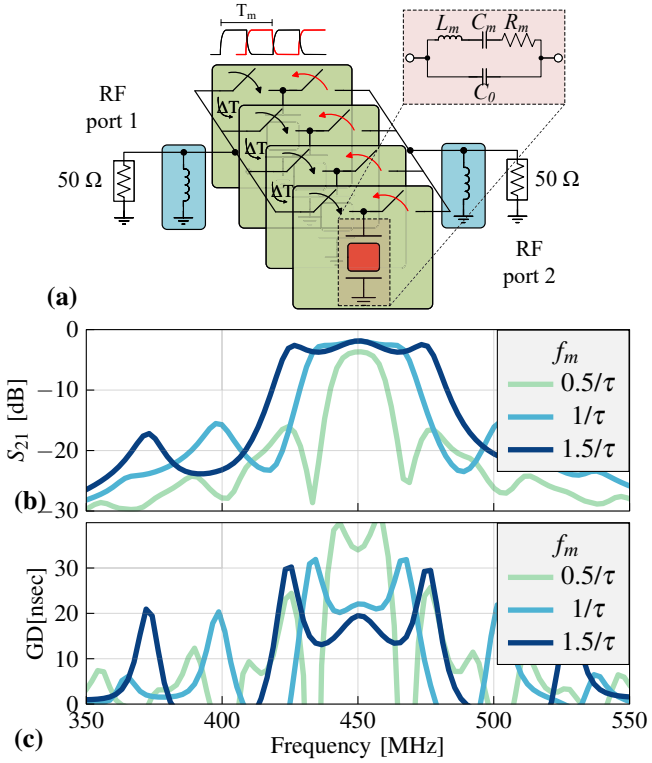

Fig. 1. Simulation results for a 4-path MEMS based MDF actuated with 50 % duty cycle signals staggered by $T_m/4$. A case scenario design using 4 identical MEMS resonators with k_t^2 =3 %, Q_m =600, f_{res} =450 MHz, Z_m =50 Ω and R_s =2 Ω is presented. Based on the calculated passive risetime of , S-parameters are shown for f_m= 8.6 MHz, 17.2 MHz and 25.7 MHz (respectively 0.5, 1, and 1.5 τ).

II. Methods

The schematic for the proposed Modulation-Defined Filter (MDF) is sketched in Fig. 1(a). An array of N cells is used to connect two RF ports through a periodic ON/OFF modulation pattern of series-connected switches, so that, within a modulation period T_m, a resonator with resonance frequency f_{res} is connected for a time DT_m (where D is the

duty cycle) to port 1 and for a time $(1-D)T_m$ to port 2. Each cell is driven with a clock skew $\Delta T = 1/NT_m$ to achieve a symmetric operation with minimized distortion. As D=0.5 for this work based on 4 cells, their phases overlap for $T_m/4$ at each port.

The signal transfer through the modulated network exhibits artificial poles: for a signal at $f_{res} \pm kf_m$, part of the input spectrum will be up/down-converted to the passive pole at f_{res}, resulting in an overall signal transfer with an infinite set of poles at $f_{res} \pm (2k+1)f_m$ obtained through modulation. In a similar way, transmission zeros are introduced at $f_{res} \pm 2kf_m$. Therefore, the proposed actuation scheme results in a dispersive delay line element, with a BW that is limited by the spacing of the first two artificial poles, so that

$$BW \approx 2f_m \tag{1}$$

For a given τ (and damping rate $f_{m,0} = 1/\tau$), one can show that a low IL can be reached at f_{res} for $f_m > f_{m,0}$. In fact, for $f_m \ll f_{m,0}$, the circuit will reach steady state for each clock period so that no signal transfer will occur. For $f_m \gg f_{m,0}$, instead, in-band ripples become larger and larger, eventually setting an upper limit to the achievable BW.

Therefore, the achievable characteristics of an MDF are mainly set by the resonator τ when loaded by a RF port. For a discrete LC resonator, $\tau_{LC} = 1/2/Q_L/\omega_{res}$, where $\omega_{res} = 2\pi f_{res}$ and Q_L is the loaded quality factor of the resonator[7]. Due to the low internal quality factors of inductor coils, Q_L below 10 leads to MDF with f_ms approaching 10 to 50 % of f_{res}. Such highs f_ms result in higher dynamic power consumption and reduced linearity, as well as ultra-wideband response 20 to 100 % BWs, orders of magnitude higher than what required in channel-selective front-ends[8], [9].

Conversely, the deployment of micro-acoustic MEMS resonators based on thin-film piezoelectric technology offer an exciting opportunity in this framework to synthesize lower fractional BWs, at reduced power consumption, maintaining high linearity and at the same time displaying interesting BW tunability features and wider BW than passive only MEMS-based ladder structures.

Starting from the conventional modified Butterworth-Van-Dyke model of piezoelectric MEMS resonators[10], it is possible to describe τ_{MEMS} for resonant input stimulus

$$\tau_{MEMS} = \frac{Z_m}{Z_0}\frac{2}{k_t^2 \omega_{res}} \tag{2}$$

if $R_m \ll Z_0$, i.e. the resonator loss is negligible with respect to the RF port impedance.

As shown, a low fractional bandwidth can be achieved thanks to the characteristic low-to-moderate k_t^2 achieved with AlN and ScAlN piezoelectric film (ranging from 1 to 10 % depending on Sc doping and excited acoustic mode [11]), and it can further be refined by proper resonator area sizing (i.e. via designing Z_m).

Using the MEMS design parameters in Fig. 1, a 58 nsec risetime is calculated via Eq. (2) and used to set the f_m range used to drive a 4-path MEMS MDF with 50 % duty-cyle. Obtained simulated S-parameters in Fig. 1-(b,c,d) show a clear BW widening mechanism as f_m increases, achieving tunable GD accordingly, at 2 to 6 % fractional f_m for k_t^2=3 %.

On one hand, the proposed filter architecture enhances the achievable BW for a given MEMS micro-acoustic technology(circa threefold in Fig. 2), when compared for the same IL(limited in both cases by any real ohmic electrode loss), providing also a real-time tunable mechanism that does not rely on varactor loading or other conventional nonlinearities that typically impair micro-acoustic filters[12].

At the same time, this platform offers exciting advantages from a technological standpoint: on one hand, it enables simplified fabrication processes, as single-frequency resonators can be deployed. On the other, smaller resonators can be designed, as 50 Ω matching is not bound to resonator area but to the conditions abovementioned, based on the circuit risetime.

Moreover, the variety of synthesizable GD (through proper sizing of the MEMS resonator but independently on k_t^2) approaches a scale that is suitable for cancelling self-interference signals resulting from backscattering in practical full-duplex RF systems, enriching the possible commercial deployment of high-Q piezoelectric resonators. For example, while a passive ladder filter with k_t^2 =3 % results in a very high delay (greater than 40 nsec), delays up to 15 nsec are achieved with MDF, and tunable via f_m (see Fig. 2).

III. Design and Fabrication of Grounded Bottom Electrode ScAlN MEMS Resonator

An array of MEMS resonators on 30 % Sc-doped AlN film devices were designed and fabricated. Due to current challenges in defining electrode patterns before ScAlN deposition, an unpatterned bottom electrode design [14] was chosen Fig. 3(e).

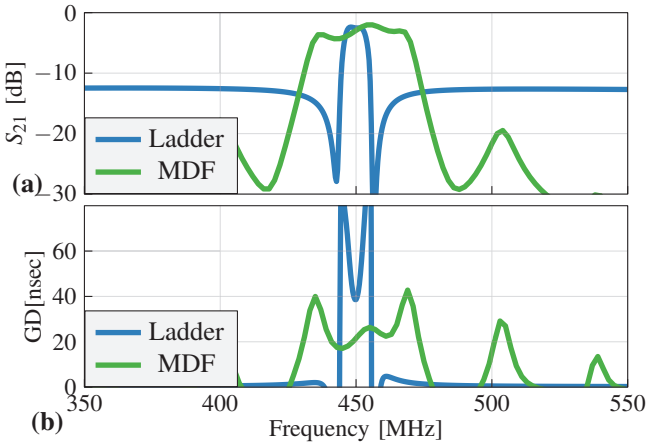

Fig. 2. Comparison of conventional 4th order MEMS ladder filter topology with the proposed 4-path MDF. The same resonator parameters of Fig. 1 are used, and identical resonator areas (leading to 50 Ω resonators) are used for the ladder filter, showcasing comparable IL(considering a 5 Ω R_{on} switch resistance), three-fold BW, higher rejection and smaller group delay (15nsec vs 60nsec at 450MHz) .

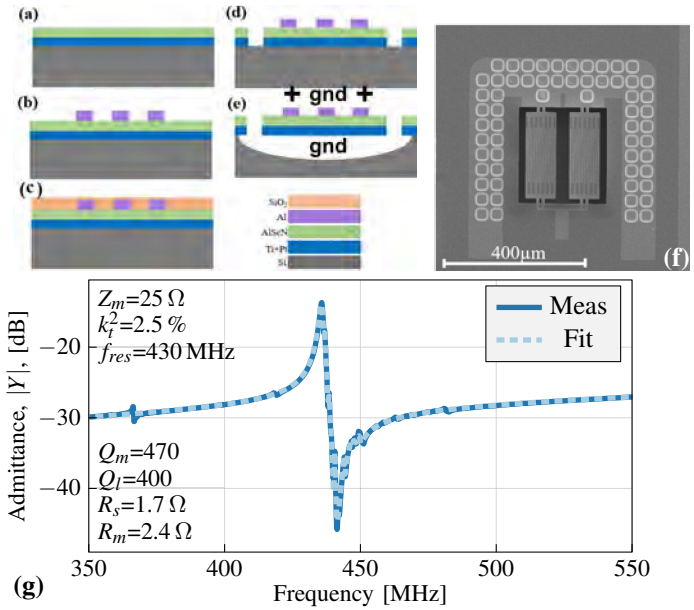

Fig. 3. (a-e) fabrication step of AlScN resonator fabrication. (f) SEM of realized device along with (g) Measured admittance response, compared to multi-modal mBVD fit of resonator perfomance, obtained with custom routine in [13]

Despite inherent k_t^2 degradation arising for poor lateral electric field coupling, a wide range of Z_m were achieved, realizing resonator with a static impedance Z_m=25 Ω at 430 MHz with overall very minimal electrode loading (Fig. 3(f)).

Resonators were built using a 4-mask fabrication process, as shown in Fig. 3(a-e). First, 10 nm of Ti and 100 nm of Pt were sputter deposited to form bottom electrode, followed without breaking vacuum by sputter deposition of AlScN with 28 % Sc and thickness target of 500 nm Fig. 3(a). Rocking curve scan revealed 1.8° FWHM, indicating good crystal quality. Vias were wet etched to connect bottom and top electrode followed by sputter deposition of 120 nm thick Al top electrode (Fig. 3(b)). Patterned SiO_2(Fig. 3(c)) layer was used as a hard mask for dry etching of AlScN trenches (Fig. 3(d)). Finally, resonators were dry released in XeF_2 plasma (Fig. 3(e)), resulting in devices in Fig. 3-(f), captured via scanning electron micrograph (SEM).

A reduction of 20 % in k_t^2 is observed due to parasitic ground coupling to the bottom electrode in the device fixture, leading to a measured k_t^2=2.5 %. While admittedly degraded with respect to AlScN-on-Si devices [15], [16], this platform provided a quick turnaround resonator technology based on ScAlN, capable of high capacity density and promising $Q \approx$ 500. Arrayed version of these devices were arranged in a common ground configuration for dicing and heterogeneous integration with RF circuitry to realize the MDF.

IV. Experimental Demonstration of MDF and SI Cancellation

A high-power handling tunable delay line for adaptive SI cancellation, enabled by micro-acoustic technologies and operating in the low VHF range (between 400 and 500 MHz) was targeted for the DARPA WARP program[17].

The above-mentioned resonator array was diced and released in a 0.5 x 2 mm die, die-attached and integrated via wire-bonds on a PCB with commercial SPDT switches by MA-COM™[18] (Fig. 4(a-b).

A measurement campaign for the assembled PCB is shown in presented in Fig. 4-(c,d). The filter response is shown for various f_m, ranging from 10 MHz (2.3 % of f_c) to 30 MHz (7 % of f_c). The achieved IL=7.5 dB is significantly degraded from 4 dB foreseen for a MEMS resonator with FoM =12 , due to the need for compensation inductors to minimize parasitic capacitance, as well as RF leakage from the SMD SPDT switch. 10 dB RL is obtained in each state for the entire band.

The MDF distortion was measured by capturing the output of the filter when a single tone at f_c (430 MHz); the first and strongest couple of cross-modulation tones were measured at $f_c \pm 4f_m$, and a suppression of 28 dBc was measured in the worst case, therefore preventing in-band distortion to corrupt SNR in practical channel-selection applications. An excellent 17 dBm $P_{1\,\mathrm{dB}}$ input linearity is reported for this prototype, limited by MEMS device linearity, limited at P_{in} >15 dBm.

We experimented on the use of the prototyped MDF as an SI canceler, given the flexibility and the reduced power

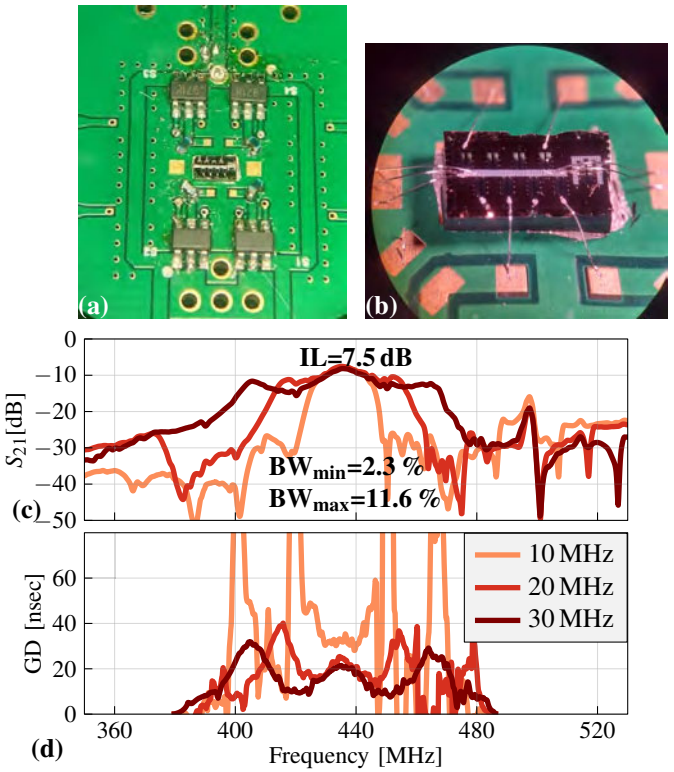

Fig. 4. (a-b)Details of the MDF prototype, built from a custom 0.5x2 mm MEMS chip, die-attached and wire-bonded to the PCB and routed to 4 SPDT COTS RF MACOM switches. (c-d) S_{21} and GD recorded for various f_m (GD windowed around 433 MHz). A peak IL of 7.5 dB is measured for resonators with FoM=12 The MDF realizes an outstanding BW tunability between 10 to 50 MHz, based on resonators with k_t^2 =2.6 %,achieved for a f_m/f_c =2.3 %, 4.6 % and 7 %, respectively.

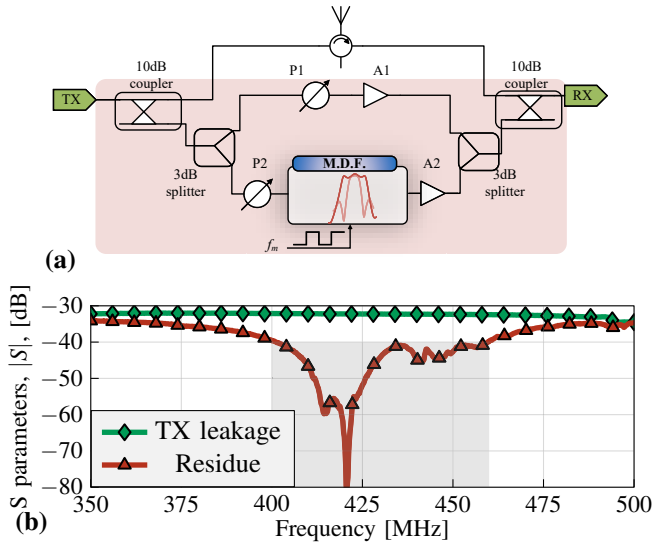

Fig. 5. (a) proposed schematic for cancellation of self-interference signal coming from TX leakage based on the MDF. (b) Measured residual from the proposed experimental setup.

consumption (10s of µW) obtained by the low-fractional f_m tunable-BW architecture, a wide range of GD and BW to cancel out TX-RX leakage in Full-Duplex systems [1].

An experimental setup was built where a TX signal is provided from the Port-1 of a Vector Network Analyzer (VNA) which is connected to the Port-1 of a COTS ferrite circulator with its Port-2 terminated by a conventional 50 Ω termination emulating a matched antenna and its Port-3 connected to the Port-2 of the VNA to capture the TX-RX leakage. A 10 dB microwave coupler is used to couple 10 dB of TX power which is split into two paths using a power splitter. These paths consist of a variable gain amplifier and phase shifter to control the gain and phase of these paths. One of the paths utilizes the MEMS resonator based delay element to provide a delay spread between the two paths. The signals from both the paths are re-combined and are injected into the RX port using a 10 dB coupler. The gains and phases of both the paths are optimized such that the SI is cancelled with the TX-RX leakage captured using the VNA is minimized thereby achieving 40 dB SI suppression over 40 MHz with at least 12 dB arising from the micro-acoustic delay of the MDF.

V. Conclusion

A technique to synthesize delay-line elements based on time-modulated cells was discussed. Performance comparisons show that by deploying MEMS resonators low-power operation, tunable BW and GD response suitable for RF signal processing, realizing BW much larger than conventional passive structures limited by piezoelectric k_t^2. A simple fabrication process was developed to demonstrate $Sc_{30}AlN$ MEMS resonator at 430 MHz, obtaining k_t^2=2.5 % and Q =500, and integrated on PCB with RF circuitry to demonstrate the proposed technique, showcasing BW up to 11.6 % with GD≈20 ns, paired with IL= 7.5 dB limited by PCB parasitics,in-band 17 dBm P_{1dB} and distortion tones lower than 28 dBc. The proposed delay line was used to realize a SI canceller for full-duplex applications. The canceller obtains 40 dB SI suppression over 40 MHz BW. Further development include the use of multiple delay lines tap to enhance the cancellation BW.

References

[1] D. Bharadia, E. McMilin, and S. Katti, "Full Duplex Radios," *SIGCOMM Comput. Commun. Rev.*, vol. 43, no. 4, pp. 375–386, Aug. 2013.

[2] J. Zhou, N. Reiskarimian, J. Diakonikolas, T. Dinc, T. Chen, G. Zussman, and H. Krishnaswamy, "Integrated Full Duplex Radios," *IEEE Communications Magazine*, vol. 55, no. 4, pp. 142–151, Apr. 2017.

[3] J. Zhou, T.-H. Chuang, T. Dinc, and H. Krishnaswamy, "Integrated Wideband Self-Interference Cancellation in the RF Domain for FDD and Full-Duplex Wireless," *IEEE Journal of Solid-State Circuits*, vol. 50, no. 12, pp. 3015–3031, 2015.

[4] G. Piazza, P. J. Stephanou, and A. P. Pisano, "Single-Chip Multiple-Frequency ALN MEMS Filters Based on Contour-Mode Piezoelectric Resonators," *Journal of Microelectromechanical Systems*, vol. 16, no. 2, pp. 319–328, 2007.

[5] A. Ghaffari, E. A. M. Klumperink, M. C. M. Soer, and B. Nauta, "Tunable High-Q N-Path Band-Pass Filters: Modeling and Verification," *IEEE Journal of Solid-State Circuits*, vol. 46, no. 5, pp. 998–1010, 2011.

[6] M. Tymchenko, D. Sounas, A. Nagulu, H. Krishnaswamy, and A. Alù, "Quasielectrostatic Wave Propagation Beyond the Delay-Bandwidth Limit in Switched Networks," *Phys. Rev. X*, vol. 9, p. 031015, Jul. 2019.

[7] R. Cameron, R. Mansour, and C. Kudsia, *Microwave Filters for Communication Systems: Fundamentals, Design and Applications*. Wiley, 2007. [Online]. Available: https://books.google.it/books?id=GyVTAAAAMAAJ

[8] C. C. W. Ruppel, "Acoustic wave filter technology–a review," *IEEE Transactions on Ultrasonics, Ferroelectrics, and Frequency Control*, vol. 64, no. 9, pp. 1390–1400, Sep. 2017.

[9] F. Hillebrand, "The Creation of Standards for Global Mobile Communication: Gsm and Umts Standardization from 1982 to 2000," *IEEE Wireless Communications*, vol. 20, no. 5, pp. 24–33, 2013.

[10] H. Bhugra and G. Piazza, *Piezoelectric MEMS Resonators*, ser. Microsystems and Nanosystems. Springer International Publishing, 2017. [Online]. Available: https://books.google.com/books?id=hYLgDQAAQBAJ

[11] V. Pashchenko, S. Mertin, F. Parsapour, J. Li, P. Muralt, and S. Ballandras, "Properties of alscn thin films for hybrid baw/saw resonator fabrication," in *2017 Joint Conference of the European Frequency and Time Forum and IEEE International Frequency Control Symposium (EFTF/IFCS)*, Jul. 2017, pp. 565–566.

[12] K.-Y. Hashimoto, S. Tanaka, and M. Esashi, "Tunable Rf Saw/baw Filters: Dream or Reality?" in *2011 Joint Conference of the IEEE International Frequency Control and the European Frequency and Time Forum (FCS) Proceedings*. IEEE, 2011, pp. 1–8.

[13] G. Michetti, "Matlab MEMS Resonator Fitting Script." [Online]. Available: https://github.com/giumc/PiezoResFitting

[14] C.-M. Lin, V. Yantchev, Y.-Y. Chen, V. V. Felmetsger, and A. P. Pisano, "Characteristics of AlN Lamb wave resonators with various bottom electrode configurations," in *2011 Joint Conference of the IEEE International Frequency Control and the European Frequency and Time Forum (FCS) Proceedings*, 2011, pp. 1–5.

[15] A. Konno, M. Sumisaka, A. Teshigahara, K. Kano, K.-y. Hashimo, H. Hirano, M. Esashi, M. Kadota, and S. Tanaka, "ScAlN Lamb wave resonator in GHz range released by XeF2 etching," in *2013 IEEE International Ultrasonics Symposium (IUS)*, 2013, pp. 1378–1381.

[16] Z. A. Schaffer, L. Colombo, A. S. Kochhar, G. Piazza, S. Mishin, and Y. Oshmyansky, "Experimental investigation of damping factors in 20% scandium-doped aluminum nitride laterally vibrating resonators," in *2018 IEEE Micro Electro Mechanical Systems (MEMS)*, Jan. 2018, pp. 787–790.

[17] DARPA, "WARP," www.darpa.mil/program/wideband-adaptive-rf-protection, 2020.

[18] MAcom, "Maswss0166rf switch," Datasheet, 2017. [Online]. Available: http://cdn.macom.com/datasheets/MASWSS0166.pdf